# Quantum chaos in weakly disordered graphene

I. Amanatidis and S. N. Evangelou*
*Department of Physics, University of Ioannina, Ioannina 45110, Greece*
(Received 18 June 2008; revised manuscript received 13 February 2009; published 21 May 2009)

We have studied numerically the statistics for electronic states (level spacings and participation ratios) from disordered graphene dots of finite size, described by the aspect ratio $W/L$ and various geometries, corresponding to finite chiral or achiral carbon nanotubes. Quantum chaotic Wigner energy level-spacing distribution is found for weak disorder, even infinitesimally small disorder for wide and short tight-binding samples ($W/L \gg 1$), while for strong disorder, Anderson localization with Poisson level-statistics always sets in. Although pure graphene near the Dirac point corresponds to integrable ballistic statistics diffusive chaotic behavior seems more common for realistic (weakly disordered) finite samples.

DOI: 10.1103/PhysRevB.79.205420 PACS number(s): 73.22.Dj, 73.63.−b, 73.20.Fz, 81.05.Uw

## I. INTRODUCTION

During the last few years theoretical and experimental interests have grown immensely on monolayer graphite samples known as graphene following its pioneering fabrication.[1–3] This remarkable two-dimensional (2D) honeycomb lattice structure made of carbon atoms behaves rather differently from ordinary 2D metals. Its most interesting quantum property is a linear dispersion near the Fermi energy, known as the Dirac point, where conduction and valence bands of graphene touch each other and the low-lying excitations behave as massless Dirac fermions.[4] Anomalous integer quantum Hall effect has been observed for graphene,[2,5] which depends on the symmetry of the introduced disorder[6] and has been discussed in terms of relativistic Dirac theory.[4,7] Due to its extraordinary properties, such as high mobility, current-carrying capacity, and thermal conduction, graphene is regarded as a good candidate to replace silicon in future nanoelectronics.[8] The possibility of gating and processing graphene sheets into multiterminal devices is also an intriguing issue for related research.[9]

The purpose of this paper is to examine the energy-level statistics and the participation ratios for finite nanotube type[10] graphene quantum dots, characterized by their aspect ratio $W/L$ (the honeycomb lattice having width $W$ and length $L$ taken in various directions), in the presence of bulk disorder. In this problem the effect of edge states, which usually appear for graphene samples in the form of nanoribbons,[4] is minimized by taking periodic boundary conditions as in nanotubes.[10] Although graphene is widely regarded as a rather clean material it is believed that various forms of weak disorder should exist,[11–16] for example, alloy type disorder from placing at random different lattice atoms or vacancies in the honeycomb lattice[14] or correlated disorder.[15] The latter, by changing the universality class from orthogonal to symplectic,[15] is expected to lead to unusual phenomena, such as weak antilocalization with metallic behavior at the Dirac point. The usual short-ranged disorder chosen here eventually causes quantum interference and Anderson localization in graphene,[16] which could limit the performance of graphene made devices.

The effects of disorder on the conduction electrons can be studied by usual scattering methods for electron waves in alternative finite structures, such as graphene billiards or flakes.[17] For pure graphene samples, near the Dirac point where the density of states vanishes, the transmission was shown to become pseudodiffusive in the limit $W/L \gg 1$ independently of boundary conditions (BC).[18] Recently,[19] a staggered potential on the edge of such terminated honeycomb lattice, which appears in LDA calculations,[20] was shown to lead to infinite-mass BC in an effective Dirac equation for the low-energy spectrum. Along this line of approach,[19] recent experimental observations showed size quantization of the electronic levels for graphene flakes[21] and led to theoretical considerations of level statistics in the tight-binding model.[22] These numerical simulations for special geometries of the honeycomb lattice, with geometrical shapes such as weakly disordered circles or triangles (named Dirac billiards[23]), were claimed to be in reasonable agreement with the observed level statistics in the experiment.[21] It was also found that weak disorder at the edges of the sample can produce quantum chaos independently of the shape of graphene dots. These calculations with level statistics mostly between integrable (Poisson) and chaotic (Wigner) did not show any signature of broken time-reversal symmetry observed in the experiment.

Here we study other sources of quantum chaos in graphene systems, such as bulk disorder, minimizing the effect of edges by choosing periodic BC as in nanotubes.[24–26] We find that the expected integrable Poisson statistics of the clean limit becomes chaotic with level repulsion for weak disorder. Moreover, our study of wide and short finite nanotube dots ($W/L \gg 1$, which is the opposite limit from the usual nanotubes), confirms the presence of pseudodiffusive behavior[18] even in the infinitesimally small disorder limit. In the opposite limit of narrow long cylinders resembling usual nanotubes ($W/L \ll 1$), the corresponding level statistics is ballistic $\delta$-function type, similar to that of the pure one-dimensional (1D) chain. Our study in the presence of disorder was not detailed enough to be able to detect the transition through the chaotic ensembles suggested in Ref. 4 by breaking the antiunitary and the time-reversal invariance. Our findings from level statistics are complemented by the participation ratio, which shows more delocalized eigenstates for weak disorder close to the Dirac point when $W/L$ is small and localized states for strong disorder and any $W/L$.

 

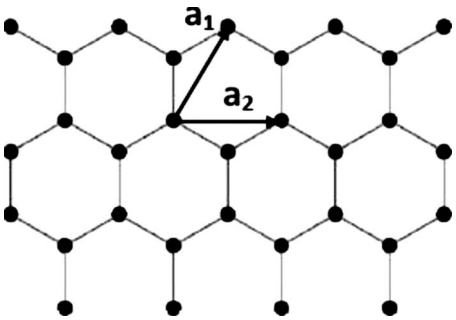


FIG. 1. The unit vectors of the graphene lattice.

The paper is organized as follows. In Sec. II we introduce the quantum dots studied. They are honeycomb lattices of various sizes and geometries, corresponding to finite length or toroidal, chiral, and achiral carbon nanotubes. Their tight-binding Hamiltonian in the presence of disorder is introduced. In Sec. III we show that for diagonal and off-diagonal disorders (in the case of large $W/L$ even for infinitesimally small disorder) Wigner chaotic level statistics is obtained while for strong disorder it always becomes Poisson, independently of the type of the graphene dot. Our results for the participation ratio complement these findings by showing more extended eigenstates close to the Dirac point for small $W/L$ and the presence of Anderson localization for strong disorder independently of $W/L$. Finally, in Sec. IV we summarize our main conclusions.

## II. TIGHT BINDING HAMILTONIAN

The tight-binding Hamiltonian of $\pi$ bonding in graphene is

$$H = \sum_i \varepsilon_i c_i^\dagger c_i - \sum_{\langle i,j \rangle} \gamma_{i,j}(c_i^\dagger c_j + c_j^\dagger c_i), \tag{1}$$

where $c_i(c_i^\dagger)$ annihilates (creates) an electron at the sites of the honeycomb lattice and $\varepsilon_i$ represents the on site energy which in the case of diagonal disorder is a random number in the range $[-w/2, w/2]$, where $w$ denotes the disorder ($\gamma_{i,j}=\gamma$). For off-diagonal disorder $\varepsilon_i=0$ and the logarithm of the nearest-neighbor hopping element $\gamma_{i,j}$ takes random values in the range $[-w/2, w/2]$.[27]

In the case of periodic BC only in one direction, the other being much longer ending with hard wall BC, the graphene dots represent finite length single wall carbon nanotubes with $W/L \ll 1$.[10] Such objects are built up by rolling sheets of graphene into very long cylinders and they are effectively one dimensional. Their electronic properties, which underpin the evolution to nanoelectronics, depend on the rolling direction. This is characterized by a set of two integers $(n,m)$ corresponding to the so-called chiral vector $\vec{C_h}=n\vec{a}_1+m\vec{a}_2$, written in terms of primitive unit lattice vectors (see Fig. 1) $\vec{a}_1=a(\frac{1}{2}, \frac{\sqrt{3}}{2})$, $\vec{a}_2=a(1,0)$, $|\vec{a}_1|=|\vec{a}_2|=\sqrt{3}a_{C-C}=a$, where $a_{C-C}$ is the distance between two atoms and $a$ the honeycomb lattice constant. Since various possibilities exist to roll up graphene, depending on the rolling direction one obtains armchair, zigzag, and chiral nanotubes.[10] The armchair nanotubes characterized by $(n,n)$ can be obtained by rolling the graphene sheet along one of the three vectors joining a honeycomb lattice site to its nearest neighbors. They are always metallic and have a perimeter which consists of $n$ hexagons connected by $n$ single bonds. The zig-zag $(n,0)$ nanotubes are defined by a rotation of the graphene sheet by 90° and the $n$ hexagons followed by $n$ single bonds lie along the longitudinal axis of the tube (the rolling direction is perpendicular). The $(n,0)$ nanotubes are metallic only when $n$ is a multiple of 3. In all other cases, that is rotating the graphene sheet in between the previous two and then rolling it up, it is equivalent to placing the hexagons followed by single bonds along intermediate directions. This third type of nanotube called chiral $(n,m)$, $n \neq m$, is metallic only when $n-m$ is a multiple of 3.[10] The hexagonal lattice symmetry guarantees that the above conclusions hold for the whole honeycomb lattice.

Our approach consists of studying the effects of disorder in the chosen graphene quantum dots by obtaining numerically the eigenvalues and eigenvectors of the Hamiltonian $H$ in the presence of disorder. In our computations we have fixed the short-ranged site (diagonal) and bond (off-diagonal) type disorders for many random samples. The statistics of the obtained eigensolutions is subsequently analyzed in order to address the quantum chaos issue. Since for the $(n,n)$ armchair nanotube a unit cell along its long direction consists of two slices around the tube (with $4n$ carbon atoms while the total number of hexagons covering the unit cell is $N_{hex}=2n$), the number of such unit cells along a finite nanotube is $N_c$ and the studied nanotube dots can be classified in terms of $n$ and $N_c$.

In the absence of disorder ($w=0$ and $\gamma_{i,j}=\gamma$) the dispersion of pure graphene sheet taken in the orientation of an armchair nanotube along the $x$ axis with its rolling direction along the vertical $y$ axis is[28]

$$E(k_x,k_y) = \pm \gamma \left[ 1 + 4\cos\left(\frac{\sqrt{3}k_y a}{2}\right)\cos\left(\frac{k_x a}{2}\right) + 4\cos^2\left(\frac{k_x a}{2}\right)\right]^{1/2}, \tag{2}$$

with quantized values of $\mathbf{k}=(k_x,k_y)$. For a finite $(n,n)$ armchair nanotube dot (periodic BC along $y$ and hard wall BC along $x$) the eigenstates are labeled by two integers via

$$k_x a = \frac{\pi}{N_c + \frac{1}{2}} j_x, \quad k_y a = \frac{2\pi}{\sqrt{3}n} j_y, \tag{3}$$

with $j_x=1,\ldots,N_c$ and $j_y=1,\ldots,2n$. The output is $2nN_c$ positive and exactly equal negative eigenvalues (a fact of sublattice symmetry,[29] since the two types of atoms A and B in graphene for nearest-neighbor hopping make two interconnected A and B sublattices). For such dots two $E=0$ modes exist only if $2N_c+1$ is a multiple of 3. In the case of infinitely long nanotubes the $k_x a$ quantization of Eq. (3) does not arise and the band structure of Eq. (2) becomes one dimensional as a function of $k_x$ only.[10] For toroidal armchair nanotube dots, where appropriate periodic BCs are imposed also along the longitudinal direction with $k_x a=\frac{2\pi}{N_c} j_x$, $j_x=1,\ldots,N_c$, four

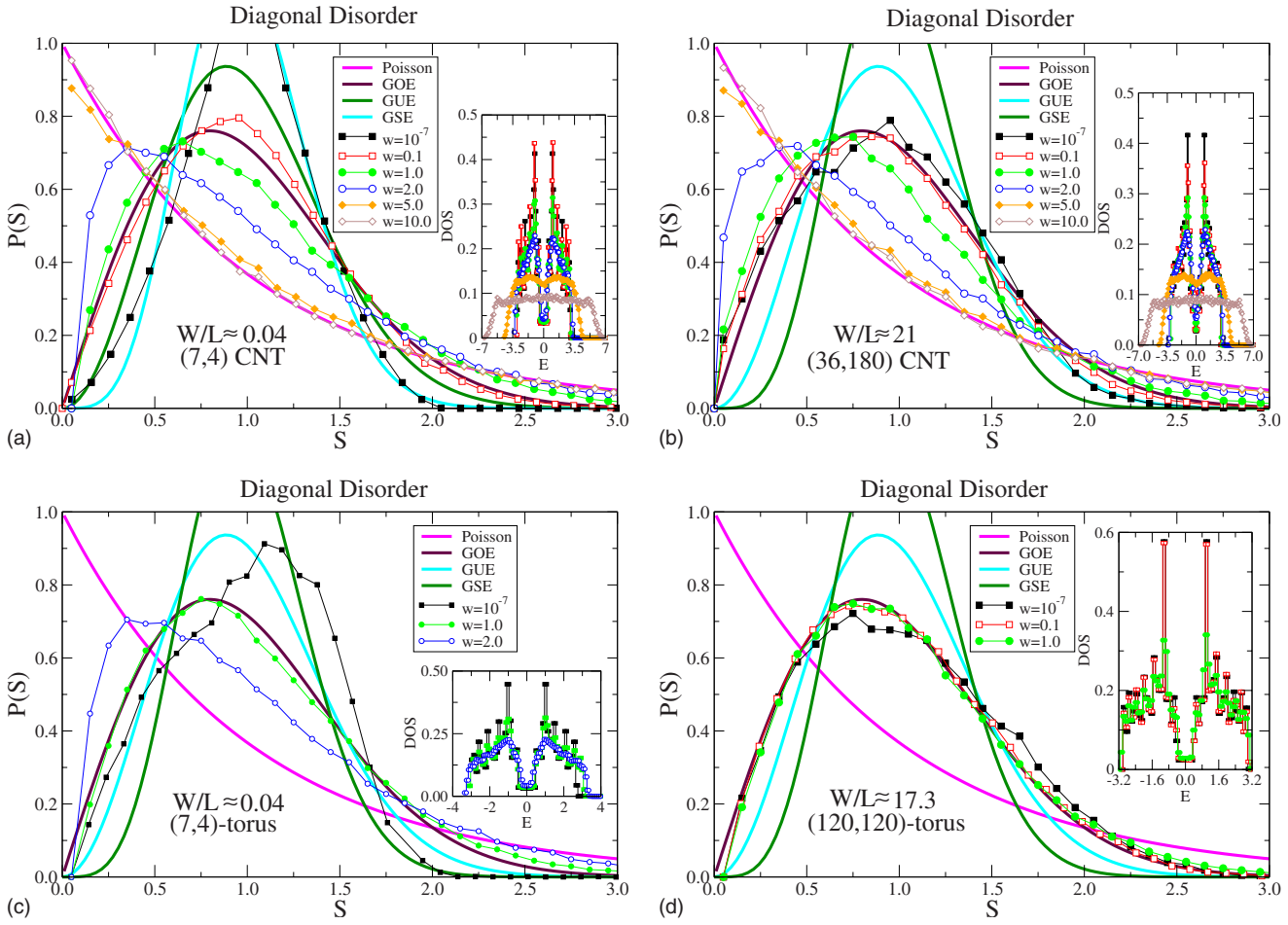


FIG. 2. (Color online) The normalized level-spacing distribution function $P(S)$ from ten samples having width $W$ and length $L$ with diagonal disorder (for the disorder strength $w$ see figure), together with the three chaotic Wigner [Gaussian orthogonal ensemble (GOE), Gaussian unitary ensemble (GUE), Gaussian symplectic ensemble (GSE)] and integrable Poisson limits: (a) For dot structures with 4960 sites and a very small aspect ratio $W/L \approx 0.04$, obtained from $N_c=40$ unit cells of the (7,4) chiral nanotube. As the disorder strength increases a gradual crossover is seen from a broad $\delta$ function (in the form of a Gaussian around the mean) for clean nanotubes to a Poisson distribution for strong disorder. (b) The same as in (a) but for wide and short ($N_c=1$ cell) structures with aspect ratio $W/L \approx 21$ (4464 sites) from a chiral (36,180) nanotube. In this case the distribution is close to Wigner even for almost zero disorder. [(c) and (d)] From $N_c=40, 12$ unit cells with 4960 and 5760 sites and aspect ratios $W/L \approx 0.04, 17.3$, obtained from the (7,4) and (120,120) toroidal nanotube geometries, respectively. The difference between the results of (c) and (d) is probably due to chirality. The corresponding densities of states are shown in insets, with the characteristic dip near the Dirac point which remains for weak disorder but closes for strong disorder ($w>3$), leading to a broad density of localized states.

$E=0$ modes exist for $N_c$ being a multiple of 3.

For the more general dots corresponding to chiral $(n,m)$, $n \neq m$, nanotubes the quantized component of the wave vector $(n,m)$ along the perimeter of the nanotube, where periodic BCs are imposed, satisfies

$$k_y a = \frac{2\pi}{W/a} j_y, \quad j_y = 1, \ldots, N_{hex}, \tag{4}$$

having width given by their perimeter $W=a\sqrt{n^2+m^2+nm}$ and $N_{hex}=2W^2/(a^2 d_r)$ hexagons in a unit cell of length $|\mathbf{T}| = \sqrt{3}W/d_r$, $d_r$ being the greatest common divisor of $2m+n$ and $2n+m$. For a given value of the quantized $k_y$ the energy of an infinite chiral nanotube dot is a function of the continuous longitudinal component $k_x$ only, with $-\frac{\pi}{|\mathbf{T}|} < k_x < +\frac{\pi}{|\mathbf{T}|}$. For armchair $(n,n)$ nanotubes the unit cell has width $W = a\sqrt{3}n$, length $|\mathbf{T}|=a$, and the number of hexagons in a unit cell is $N_{hex}=2n$. For $N_c$ unit cells of a chiral $(n,m)$ nanotube the dot length is $L=N_c|\mathbf{T}|$ and the considered aspect ratio $W/L=d_r/(\sqrt{3}N_c)$, which reduces to $W/L=\sqrt{3}n/N_c$ for $(n,n)$ armchair nanotube dots.

The participation ratio for each eigenstate of energy $E$ is defined in terms of normalized amplitudes over all lattice sites by the sum $(\Sigma_j |\psi_j(E)|^4)^{-1}$. It is a non-self-averaging quantity alternative to the usual localization length, which was studied for nanotubes by scattering techniques producing interesting results.[24–26]

## III. RESULTS

### A. Pure graphene sheets

In the absence of disorder the eigensolutions can be easily obtained, also for chiral nanotubes where their unit cell along

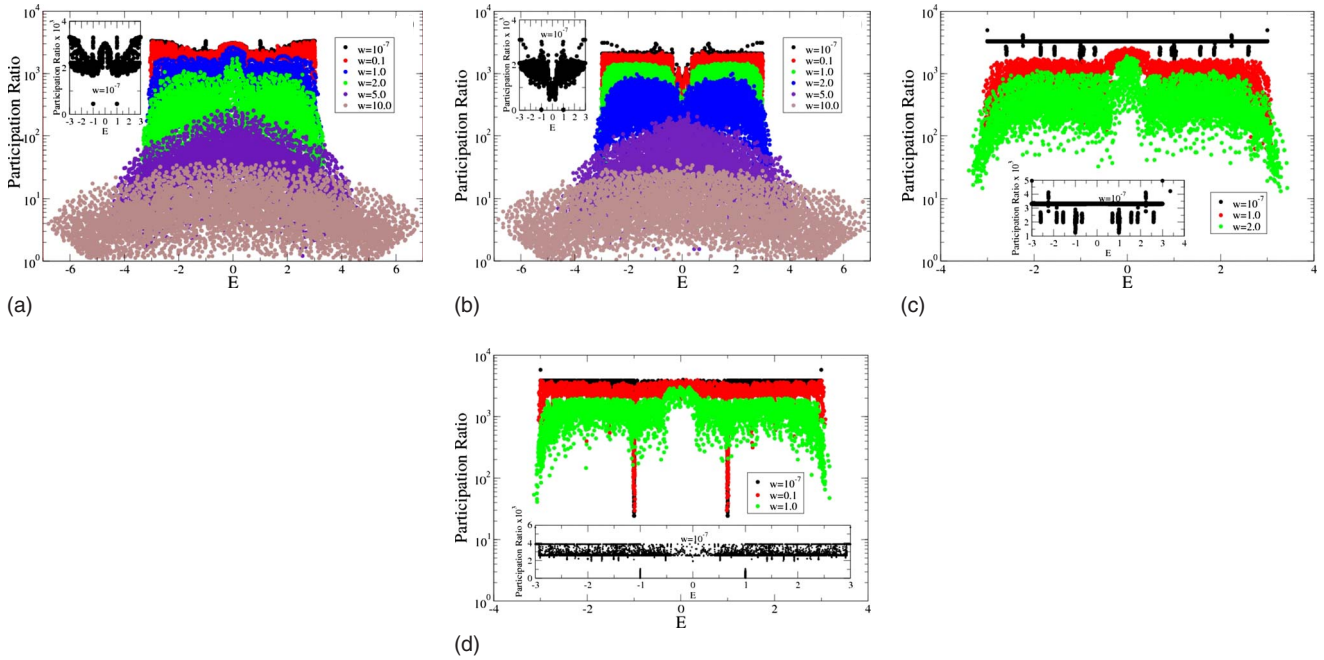


FIG. 3. (Color online) The participation ratios of the corresponding eigenstates vs energy for the same parameters as in Fig. 1. They indicate the number of sites where each eigenstate has significant amplitude. For a perfectly extended state, spreading to all sites of the chosen lattice, the participation ratio should be ≈5000. Our magnified results for pure graphene ($w=0$) are shown in insets (note the linear scale on the $y$ axis).

the tube can become arbitrarily large depending on $(n,m)$. For pure graphene dots and arbitrary $W/L$ the expected behavior is integrable Poisson statistics, which becomes ballistic 1D-like in the limit $W/L \ll 1$. This can be simply understood near the Dirac point where the density of states is linear. In this regime the integrated density of states is $\mathcal{N}(E) \propto E^2$. Therefore, the statistics of the energy levels $E$ should be replaced by the statistics of the unfolded squared levels $E^2$, which is required in order to have constant density of states with fixed mean level spacing. If we use the usual quadratic dispersion for the squared levels $E^2 \propto k_x^2 + k_y^2$ the statistic near the Dirac point becomes equivalent to the statistics of integrable billiards,[30] with $E^2$ replaced by $E$ from

$$E_{j_x,j_y} = \alpha j_x^2 + j_y^2, \quad j_x,\ j_y \ \text{integers}, \tag{5}$$

with $\alpha$ being an irrational number fixed by the size of the adopted sample. The $E$'s from Eq. (5), which have a constant density of states near the Dirac point, obviously give Poisson level statistics,[30] except for very long samples where the sum of Eq. (5) reaches the 1D limit and should depend on one parameter only so that the corresponding level statistics if $W/L \ll 1$ becomes a trivial $\delta$ function.

Although we have verified that a broad $\delta$ function holds for small $W/L$ [e.g., by adding infinitesimally small disorder is shown in Fig. 2(a), which denotes the expected trivial $1D$-like ballistic behavior], we find a different result for large $W/L$. In this case statistics becomes chaotic even for almost pure systems [e.g., see the Wigner distribution shown in Fig. 2(b)]. Therefore, in the almost clean limit the ballistic behavior is valid only for small $W/L$ and is replaced by a chaotic curve when raising the aspect ratio $W/L$. In the chaotic case a more dominant role is given to the abrupt edges, which add strong intervalley scattering.

In the insets of Fig. 3 the behavior of the corresponding eigenstates of pure graphene dots can be seen via their participation ratios. The main observation is that for the small $W/L$ [Fig. 3(a) inset] the majority of ballistic states have a higher participation ratios when compared to those with large $W/L$ [Fig. 3(b) inset]. The distribution of the participation values becomes sharper for the small $W/L$ toroidal nanotube dots [Fig. 3(c) inset] when compared to large $W/L$ (Fig. 3(d) inset). For toroidal nanotube dots BCs exist in both directions and small $W/L$ is the same as large $W/L$, so that only chirality from the orientation of the lattice probably plays a role. In this case the behavior of Fig. 3(b) near the Dirac point is absent.

### B. Diagonal and off-diagonal disorders

The density of states and the level-spacing distribution function $P(S)$ are computed for various graphene dots with aspect ratios $W/L$, including chiral nanotube dots. The corresponding nearest-level-spacing distribution function is illustrated for different values of diagonal disorder in Fig. 2. All the unfolded energy levels in the band are considered for 10 runs, requiring the density of states to be constant everywhere in the band. No significant difference was found when levels near the Dirac point are considered only. For small $W/L$ [Fig. 2(a)] the level-spacing distribution function $P(S)$ is shown to vary from a broad $\delta$-function-like curve for almost zero disorder ($w=10^{-7}$) toward the Poisson localized limit for strong disorder $w$. For large $W/L$ we observe instead [Fig. 2(b)] a crossover not from a $\delta$ function but from

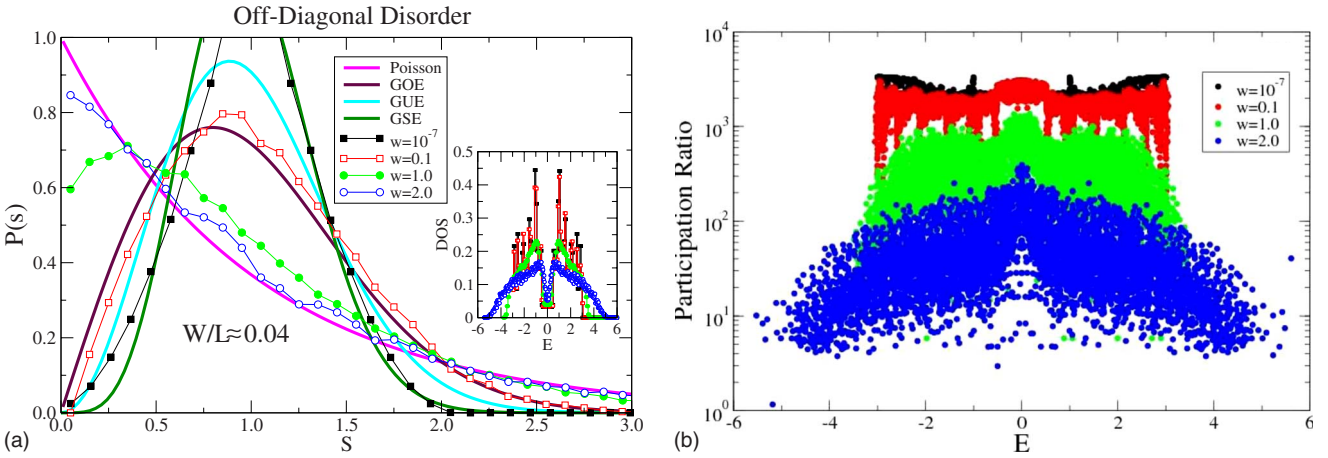


FIG. 4. (Color online) (a) The level-spacing distribution function $P(S)$ and (b) the participation ratio for off-diagonal disorder of strength $w$ (see figure) for the small aspect ratio $W/L \approx 0.04$ chiral (7,4) nanotube geometry of $N_c=40$ cells (4960 sites).

a Wigner chaotic distribution toward the localized Poisson limit in the strong disorder $w$. In the insets of Fig. 2 the corresponding average density of states is shown with the dip near the Dirac point, which disappears when the disorder increases beyond a certain value.

In Fig. 3 we demonstrate the participation ratio which measures the extent of the corresponding eigenstates on the chosen lattices. Near the Dirac point the values are seen to be higher for small $W/L$ [Fig. 3(a)] when compared to large $W/L$ [Fig. 3(b)]. This observation is related to the observed $\delta$ function and Wigner $P(S)$ distributions of Fig. 2 for small and large $W/L$, respectively. Similar results, shown in Figs. 3(c) and 3(d), are obtained for toroidal nanotube dots. For strong disorder they indicate localization of all the states in the band with their participation ratio becoming small.

Off-diagonal disorder is certainly different since it preserves chiral symmetry by connecting one sublattice to the other.[29] In Fig. 4 we show our results for the chiral (7,4) nanotube with off-diagonal disorder in the small $W/L \ll 1$ limit. Figure 4(a) shows $P(S)$ (with the density of states in the inset) and Fig. 4(b) shows the participation ratio of the corresponding eigenstates. The results are similar to the diagonal disorder case, with the exception of the appearance of a singularity in the density of states, which develops at the band center (not seen in the figure due to scale).[27]

## IV. DISCUSSION

Our study of the eigensolution statistics of nanotube quantum dots in the presence of disorder, for various finite geometries specified by the aspect ratio $W/L$, reveals some interesting features. First, quantum chaos becomes relevant also for weakly disordered graphene, with pseudodiffusive Wigner statistics even for almost zero disorder when $W/L$ is large. Second, for strong disorder localization occurs for all states in the band, in agreement with finite-size scaling transfer-matrix studies at the Dirac point. Third, near the Dirac point, due to the linearity of density of states of pure graphene, a natural unfolding of levels which makes the density of states constant corresponds to the study of squares of energies $E^2$ (instead of $E$ with linearly vanishing density) which gives integrable irrational billiard Poisson statistics. However, since infinitesimal disorder is inevitable the question of whether ballistic or diffusive behavior prevails near the Dirac point can be answered in favor of a simple 1D-like ballistic behavior for small $W/L$ and chaotic for large $W/L$.

In conclusion, our computations for finite graphene quantum dots in the presence of weak disorder show quantum chaos. This demonstration in graphene nanotube dots is consistent with experimental studies of graphene flakes[21] although more elaborate computations are required for graphene nanotube dots and graphene flakes in order to display the transition through GSE and GUE expected from symmetries. Therefore, in realistic graphene samples the outstanding ballistic behavior of long carbon nanotubes will probably be replaced by diffusive chaotic behavior for short and wide nanotube dots even with arbitrary small disorder.

*sevagel@cc.uoi.gr

[1] K. S. Novoselov, A. K. Geim, S. V. Morozov, D. Jiang, Y. Zhang, S. V. Dubonos, I. V. Grigorieva, and A. A. Firsov, Science **306**, 666 (2004).
[2] K. S. Novoselov, A. K. Geim, S. V. Morozov, D. Jiang, M. I. Katsnelson, I. V. Grigorieva, S. V. Dubonos, and A. A. Firsov, Nature (London) **438**, 197 (2005).
[3] A. K. Geim and K. S. Novoselov, Nature Mater. **6**, 183 (2007).
[4] C. W. J. Beenakker, Rev. Mod. Phys. **80**, 1337 (2008).
[5] Y. Zhang, Y. W. Tan, H. L. Stormer, and P. Kim, Nature (London) **438**, 201 (2005).
[6] P. M. Ostrovsky, I. V. Gornyi, and A. D. Mirlin, Phys. Rev. B **77**, 195430 (2008).
[7] V. P. Gusynin and S. G. Sharapov, Phys. Rev. Lett. **95**, 146801 (2005).
[8] C. Berger, Z. Song, X. Li, X. Wu, N. Brown, C. Naud, D. Mayou, T. Li, J. Hass, A. N. Marchenkov, E. H. Conrad, P. N. First, and W. A. de Heer, Science **312**, 1191 (2006).

[9] C. Berger, Z. Song, T. Li, X. Li, A. Y. Ogbazghi, R. Feng, Z. Dai, A. N. Marchenkov, E. H. Conrad, P. N. First, and W. A. de Heer, J. Phys. Chem. B **108**, 19912 (2004).
[10] R. Saito, G. Dresselhaus, and M. S. Dresselhaus, *Physical Properties of Carbon Nanotubes* (Imperial College Press, London, 1998).
[11] J. C. T. White and T. N. Todorov, Nature (London) **393**, 240 (1998).
[12] M. Hjort and S. Stafstrom, Phys. Rev. B **63**, 113406 (2001).
[13] A. Altland, Phys. Rev. Lett. **97**, 236802 (2006).
[14] N. M. R. Peres, F. Guinea, and A. H. Castro Neto, Phys. Rev. B **73**, 125411 (2006).
[15] P. M. Ostrovsky, I. V. Gornyi, and A. D. Mirlin, Eur. Phys. J. Spec. Top. **148**, 63 (2007).
[16] S.-J. Xiong and Y. Xiong, Phys. Rev. B **76**, 214204 (2007).
[17] F. Miao, S. Wijeratne, Y. Zhang, U. C. Coskun, W. Bao, and C. N. Lau, Science **317**, 1530 (2007).
[18] J. Tworzydlo, B. Trauzettel, M. Titov, A. Rycerz, and C. W. J. Beenakker, Phys. Rev. Lett. **96**, 246802 (2006).
[19] A. R. Akhmerov and C. W. J. Beenakker, Phys. Rev. B **77**, 085423 (2008).
[20] M. Wimmer, I. Adagideli, S. Berber, D. Tomanek, and K. Richter, Phys. Rev. Lett. **100**, 177207 (2008).
[21] L. A. Ponomarenko, F. Schedin, M. I. Katsnelson, R. Yang, E. W. Hill, K. S. Novoselov, and A. K. Geim, Science **320**, 356 (2008).
[22] H. De Raedt and M. I. Katselson, Pis'ma Zh. Eksp. Teor. Fiz. **88**, 698 (2008).
[23] M. V. Berry and R. J. Mondragon, Proc. R. Soc. London, Ser. A **412**, 53 (1987).
[24] Blanca Biel, F. J. Garcia-Vidal, Angel Rubio, and Fernando Flores, Phys. Rev. Lett. **95**, 266801 (2005).
[25] R. Avriller, S. Roche, F. Triozon, X. Blase, and S. Latil, Mod. Phys. Lett. B **21**, 1955 (2007).
[26] N. Nemec, K. Richter, and G. Cuniberti, New J. Phys. **10**, 065014 (2008).
[27] S. N. Evangelou and D. E. Katsanos, J. Phys. A **36**, 3237 (2003).
[28] C. Bena and G. Montambaux, arXiv:0712.0765 (unpublished).
[29] M. Inui, S. A. Trugman, and E. Abrahams, Phys. Rev. B **49**, 3190 (1994).
[30] G. Casati, B. V. Chirikov, and I. Guarneri, Phys. Rev. Lett. **54**, 1350 (1985).